LETTERS
PUBLISHED ONLINE: 3 JULY 2011 | DOI: 10.1038/NMAT3053
nature materials

Controlled enhancement of spin-current emission by three-magnon splitting

Hidekazu Kurebayashi[1]*, Oleksandr Dzyapko[2], Vladislav E. Demidov[2], Dong Fang[1], A. J. Ferguson[1] and Sergej O. Demokritov[2]

Spin currents—the flow of angular momentum without the simultaneous transfer of electrical charge—play an enabling role in the field of spintronics[1–8]. Unlike the charge current, the spin current is not a conservative quantity within the conduction carrier system. This is due to the presence of the spin–orbit interaction that couples the spin of the carriers to angular momentum in the lattice. This spin–lattice coupling[9] acts also as the source of damping in magnetic materials, where the precessing magnetic moment experiences a torque towards its equilibrium orientation; the excess angular momentum in the magnetic subsystem flows into the lattice. Here we show that this flow can be reversed by the three-magnon splitting process and experimentally achieve the enhancement of the spin current emitted by the interacting spin waves. This mechanism triggers angular momentum transfer from the lattice to the magnetic subsystem and modifies the spin-current emission. The finding illustrates the importance of magnon–magnon interactions for developing spin-current based electronics.

By using angular momentum exchanges between conduction electrons and spin waves, the long-range transport of spin current has recently been demonstrated in magnetic insulators[8], finding an important role for these materials within spin-based electronic devices. To create and detect the spin current, layers of a metal with a strong spin–orbital coupling (Pt) were placed on the magnetic insulator (yttrium iron garnet, YIG). Passing a current through the metal layer generates a spin current, by means of the spin-Hall effect (SHE)[10,11]. The spin current is injected into the magnetic dielectric, where it results in an excitation of a propagating spin wave. After propagation for a certain distance, the spin angular momentum of the spin wave is converted into a voltage in the second metal layer by means of the inverse spin-Hall effect (ISHE; ref. 7). This signal-transmission scheme has advantages over the conceptually simpler approach of using spin-polarized electrons in conducting materials, owing to the longer propagation length of spin waves relative to the spin-diffusion length in metals. Whereas the spin-diffusion length of conduction carriers in metals is normally several hundreds of nanometres[12], spin waves in magnetic dielectrics such as YIG can propagate to macroscopic distances without significant attenuation as a result of the very small magnetic damping in this material[13]. The performance of such a signal transmission scheme is mainly limited by the conversion efficiency of a spin current into the magnetization precession and vice versa. As the output voltage in this scheme is directly proportional to the spin current flowing across the interface between the magnetic dielectric and the metal film, the way to improve the performance of the scheme is to find a mechanism for an efficient enhancement of the spin current. Here we demonstrate that such enhancement can be realized by using the three-magnon splitting process, a magnon–magnon interaction in which the total angular momentum of the magnetic subsystem is not conserved. Moreover, we show that this mechanism can be switched on and off by modification of the spin-wave spectrum in YIG by the applied static magnetic field.

Figure 1a is a schematic of the studied system, which consists of a bilayer of a magnetic insulator YIG and a spin-current detector Pt. We first characterize the magnetic properties of the YIG film using a ferromagnetic resonance (FMR) technique. Figure 1b demonstrates the dependence of microwave absorption on the magnetic field measured for a fixed excitation frequency $f = 5\,\mathrm{GHz}$. The absorption curve is asymmetric and exhibits a maximum at the field H_{res}. This asymmetry is most likely due to the contribution of different standing spin-wave modes[14]. The maximum of the curve corresponds to the fundamental spin-wave mode of the finite-size YIG sample, being an analogue of the uniform FMR mode in an infinite ferromagnetic medium. The connection between the resonant field of this mode H_{res} and the frequency f can be approximated with a good accuracy by the Kittel formula[15] $f = \gamma\mu_0\sqrt{H_{\mathrm{res}}(H_{\mathrm{res}}+M)}$, where $\gamma = 28\,\mathrm{GHz\,T^{-1}}$ is the gyromagnetic ratio and $\mu_0 M = 0.175\,\mathrm{T}$ is the saturation magnetization of YIG (Fig. 1c). The voltage detected across the Pt film also shows resonance-like behaviour, with a maximum at H_{res}. To prove whether the observed voltage is actually caused by the ISHE and that it can be used as a measure of the spin current, we performed these measurements for three different directions of the static field $\mathbf{H}_0$, as shown in Fig. 1d. Considering the most important flow of the longitudinal magnetization (that is along $\mathbf{H}_0$), voltages arising from the ISHE follow the symmetry of conversion from a spin current $\mathbf{j}_s$ into electromotive force $\mathbf{E}$ as[7]:

$$\mathbf{E} = D_{\mathrm{ISHE}}\mathbf{j}_s \times \boldsymbol{\sigma} \qquad (1)$$

where D_{ISHE} and $\boldsymbol{\sigma}$ are the conversion efficiency and the unit vector in the direction of the spin polarization of $\mathbf{j}_s$, respectively. As defined in Fig. 1a, the directions of $\mathbf{E}$ and $\mathbf{j}_s$ for our set-up are fixed along the y and x direction respectively, and the direction of $\boldsymbol{\sigma}$, being parallel to $\mathbf{H}_0$ in the in-plane measurements, can be experimentally controlled. In agreement with equation (1), we observed the voltage only when $\mathbf{H}_0$ was applied along the z-axis with a corresponding sign change and no sizeable voltage was measured for $\mathbf{H}_0$ parallel/antiparallel to the y axis.

We now analyse the frequency dependence of the resonant peak voltage ΔV when applying $\mathbf{H}_0$ along the z-axis. For each value of the excitation frequency the static magnetic field was

---

[1]Cavendish Laboratory, University of Cambridge, J. J. Thomson Avenue, CB3 0HE, UK, [2]Institute for Applied Physics, University of Muenster, Corrensstr. 2-4, 48149 Muenster, Germany. *e-mail: hk295@cam.ac.uk.

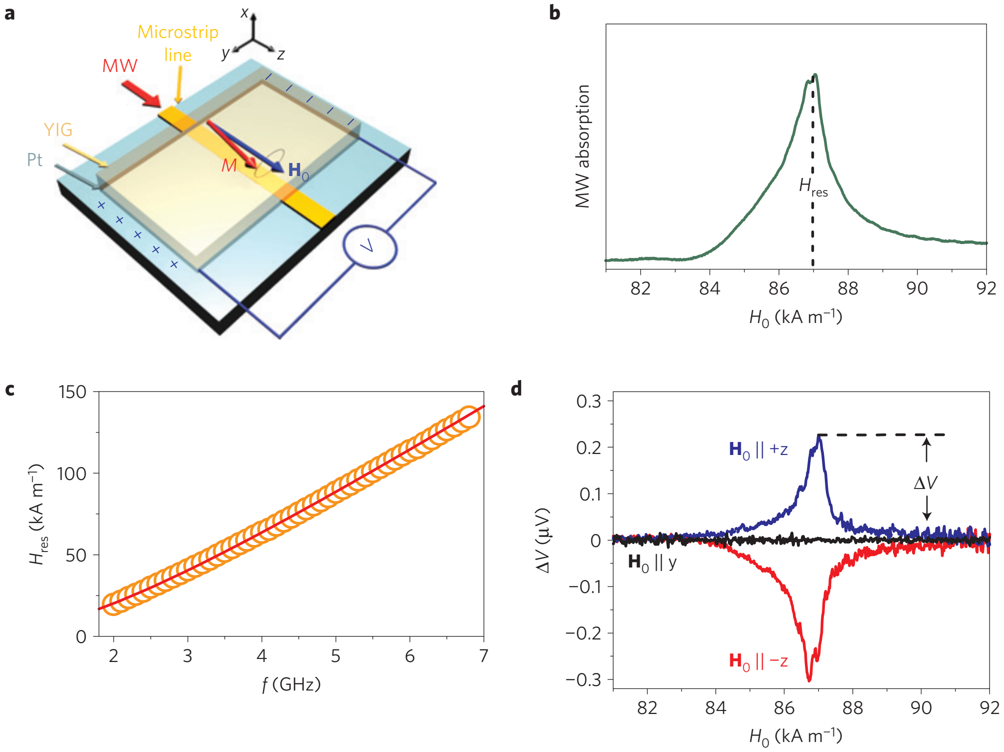

Figure 1 | Ferromagnetic resonance and spin-current detection in YIG/Pt layered system. a, Schematic layout of the experimental set-up. Ferromagnetic resonance in the YIG layer is excited using a microwave current (MW) flowing in a microstrip transmission line. $\mathbf{H}_0$ denotes the applied static magnetic field and M denotes magnetization. Electrodes attached to the Pt film are used to detect the voltage induced in the film due to the flow of spin current. **b**, Ferromagnetic resonance in YIG at $f = 5$ GHz detected by means of microwave absorption for $\mathbf{H}_0 \parallel \mathbf{z}$. H_{res} defines the resonance field. **c**, Frequency dependence of H_{res} for $\mathbf{H}_0 \parallel \mathbf{z}$, the circles indicate the experimental data and the solid curve is calculated based on the Kittel formula. **d**, Field dependence of the induced voltage measured at different orientations of $\mathbf{H}_0$, as labelled. ΔV indicates the peak value of V at H_{res}.

adjusted to keep the system at resonance, so that the mode excited by microwaves is the quasi-uniform FMR mode of the YIG sample. As seen in Fig. 2a, a nearly constant ΔV is observed for frequencies larger than 3.2 GHz. Surprisingly, below 3.2 GHz there is an abrupt increase in ΔV. To prove whether this increase is associated with increased microwave absorption power P_{abs}, which characterizes the angular momentum transferred from the microwave field to the magnetic subsystem, we measured the frequency dependence of P_{abs} (shown in Fig. 2b). The experimental data indicate that P_{abs} does not increase, but rather decreases, for $f < 3.2$ GHz, which can be explained by the reduction of magnetic susceptibility in YIG. Therefore, one can conclude that the observed increase of ΔV (and that of $\mathbf{j}_{\mathrm{s}}$) is not due to the change of the microwave absorption. To take into account the frequency dependence of P_{abs}, we introduce $\Delta V/P_{\mathrm{abs}}$, a parameter that characterizes the conversion efficiency of the angular momentum created by the microwave field into the spin current $\mathbf{j}_{\mathrm{s}}$ (ref. 14). As seen in Fig. 2c, starting from $f =$ 3.2 GHz, the conversion efficiency continuously increases with decreasing frequency. Similar experiments performed keeping the absorbed microwave power constant (see the inset of Fig. 2c) also demonstrate a clear enhancement of the ISHE voltage at $f < 3.2$ GHz. As the absorbed power is proportional to the injected angular momentum from the microwave source, we can confirm that the reduction of P_{abs} is the origin of the decrease in ΔV observed below 3.0 GHz in Fig. 2a. These experimental findings suggest that for $f < 3.2$ GHz the magnetic subsystem absorbs the angular momentum from a source other than the microwave field. In agreement with this assumption, the linear excitation theory describing the interaction of the magnetic subsystem with the microwave field[16–18] (see Supplementary Information) was found to be applicable to the experimental data only for $f > 3.2$ GHz (solid line in Fig. 2c). To characterize the observed enhancement at different applied microwave powers P, we analysed the ratio of ΔV measured at frequencies above (4 GHz) and below (3 GHz) the critical frequency 3.2 GHz as a function of P (Fig. 2d). The enhancement of ΔV is more efficient at low powers and gradually disappears with increasing P. Thus, the increase of ΔV can be attributed to a nonlinear spin-wave process (see Supplementary Information).

To obtain additional information about the magnetic subsystem, we used Brillouin light scattering (BLS) spectroscopy[19]. This technique is sensitive not only to the quasi-uniform FMR mode, but also to short-wavelength spin waves, which can be created by the relaxation of magnetization dynamics. Figure 3 shows the BLS intensity as a function of the excitation and detection frequencies. The data were obtained by maintaining the system at resonance and the detection frequency corresponds to the frequency of spin waves in the YIG layer. At excitation frequencies above 3.2 GHz, the BLS spectrum shows peaks at an FMR frequency that is equal to the excitation frequency (solid line in the figure). At lower excitation frequencies, however, a second group of spin waves occurs in the spectrum, with frequencies that are exactly one half of the excitation frequency (dashed line in the figure). These additional spin waves are created as a result of the three-magnon splitting process[13,20,21], representing a splitting of the quasi-uniform FMR mode into two short-wavelength spin waves of the half frequency, as illustrated in the inset of Fig. 3. This process is allowed only if there are available spectral states at the frequency of the secondary spin waves. As a result of the peculiarities of the spin-wave spectrum in ferromagnets[13], this condition is met only for relatively small static magnetic fields

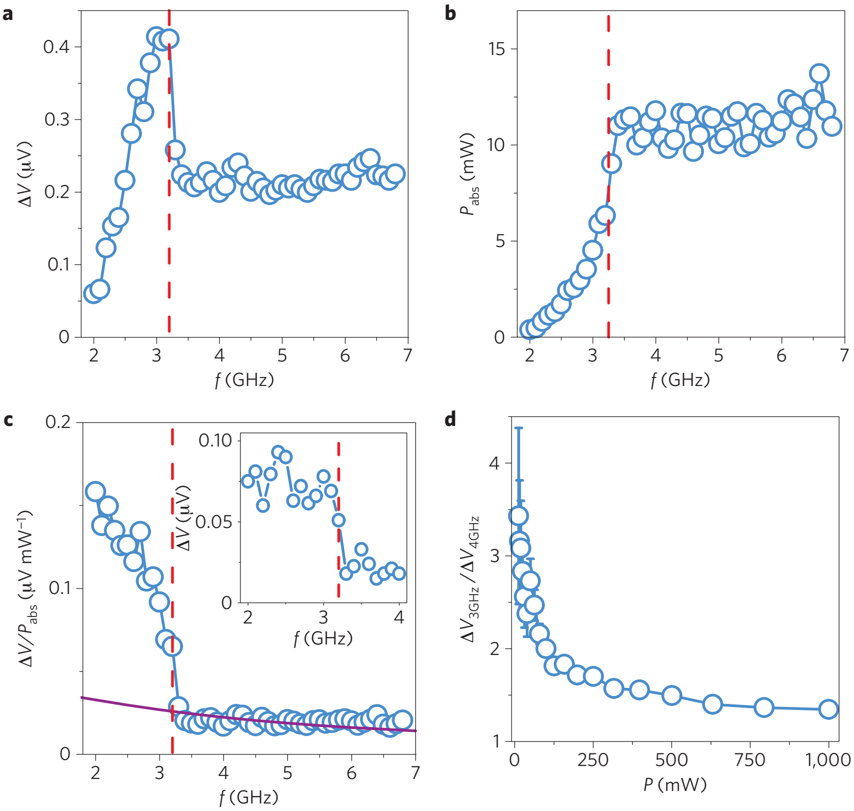

Figure 2 | The frequency and power dependence of the ISHE voltage and the microwave absorption in YIG. a, Frequency dependence of the peak voltage at resonance conditions. Note that an abrupt increase of ΔV is observed at $f < 3.2$ GHz (red dashed line). **b**, Frequency dependence of the absorbed microwave power. A strong decrease of P_{abs} starts at $f = 3.2$ GHz (red dashed line). **c**, Frequency dependence of the ratio $\Delta V/P_{abs}$, which characterizes the conversion efficiency of the angular momentum absorbed from microwaves into spin current, measured at a constant power of microwave excitation. A strong increase of $\Delta V/P_{abs}$ starts at $f = 3.2$ GHz (red dashed line). The solid line is the result of calculations based on the linear excitation theory. The inset shows the results of similar measurements performed by keeping the absorbed microwave power (P_{abs}) constant. **d**, Power dependence of the enhancement of spin current, characterized by the ratio of the values of ΔV measured 3.0 and 4.0 GHz. The strong power dependence indicates that a nonlinear process is behind the enhancement.

(therefore low excitation frequencies). Calculations based on the spin-wave theory in magnetic films[22] show that the three-magnon splitting is allowed in YIG for FMR frequencies below 3.15 GHz, which matches well with the experimental value of the critical frequency (3.2 GHz).

These results reveal a clear correlation between the enhancement of the spin current observed at low frequencies and the three-magnon splitting process. The three-magnon splitting is well known[23] and usually considered as a parasitic effect, limiting the performance of conventional microwave electronic devices. Furthermore, in proposed spin-wave electronics[24] employing the inductive technique for detection of magnetization oscillations, it is difficult to detect and use the short-wavelength secondary spin waves. By contrast, in spin-current devices based on the angular momentum exchange at interfaces, both quasi-uniform FMR and short-wavelength spin waves contribute to the signal conversion. To understand the effect of the three-magnon splitting on the spin current let us discuss the flow of angular momentum in the studied system illustrated in Fig. 4. It is important to emphasize that, because of angular momentum conservation, any changes of magnetization in a ferromagnet result in changes of the angular momentum accumulated in the magnetic subsystem. Thus, to change the magnetization, one needs to create a corresponding flow of the angular momentum between the magnetic subsystem and an external source (for example, the lattice), as happens in the Einstein–de Haas effect[25]. In the absence of three-magnon splitting (Fig. 4a), the source of the angular momentum flow causing the excitation of the magnetization precession is the flow from the microwave field $\mathfrak{T}_{\mathrm{MW}}$. This precession leads to the reduction of the longitudinal magnetization $\Delta \mathrm{M}_{\parallel}$. At equilibrium, the flow from the microwave field is balanced by the flow of the angular momentum into the lattice $\mathfrak{T}_{\mathrm{L}}$ due to the spin–lattice relaxation: $\mathfrak{T}_{\mathrm{MW}} = \mathfrak{T}_{\mathrm{L}}$. Using the Bloch equation[7], $\Delta \mathrm{M}_{\parallel}$ is expressed as $\Delta \mathrm{M}_{\parallel} = \gamma \mathfrak{T}_{\mathrm{L}} T_1$, where T_1 is the spin–lattice relaxation time. In the presence of the Pt layer, we should take into account an additional flow due to the spin current $\mathbf{j}_{\mathrm{s}}$ across the YIG/Pt interface, which is also proportional to $\Delta \mathrm{M}_{\parallel}$ (refs 8,16–18), by replacing T_1 with an effective time T_1^* ($T_1^* < T_1$). Thus, the flow equilibrium between the microwave field, on one side, and the lattice and Pt layer, on the other side, defines the equilibrium value of $\Delta \mathrm{M}_{\parallel}$ and therefore that of $\mathbf{j}_{\mathrm{s}}$, both of which are proportional to T_1^*. We emphasize that the only source of the angular momentum is the microwave field and both $\mathbf{j}_{\mathrm{s}}$ and ΔV are defined solely by the absorbed microwave power, as $\Delta \mathrm{M}_{\parallel} \propto \mathrm{P}_{\mathrm{abs}}$.

The situation changes drastically when three-magnon splitting is involved, as illustrated in Fig. 4b. The quasi-uniform FMR mode excited by the microwave field creates short-wavelength spin waves as a result of the three-magnon splitting. Then both the quasi-uniform FMR and the spin waves transfer the angular momentum into the lattice and to the Pt layer. At first glance, it seems that the total flow equilibrium is not affected, because the microwave field remains the only source of the angular momentum. However, this is the case only if the three-magnon splitting were to conserve the total angular momentum of the magnetic subsystem.

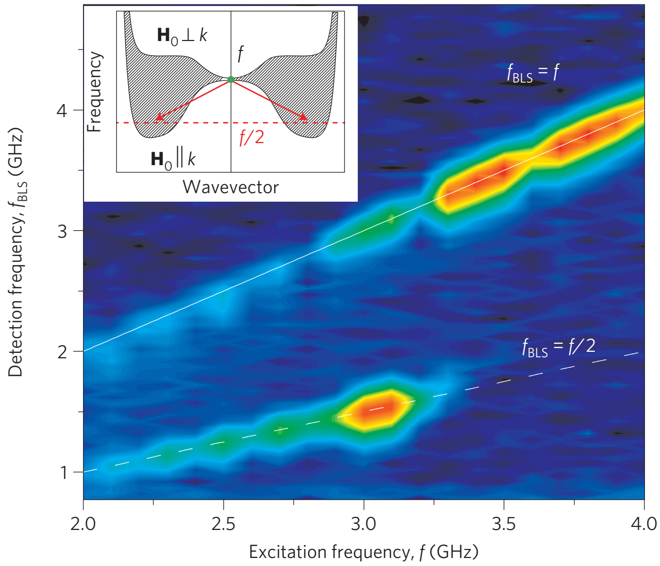

Figure 3 | Spin waves created by the three-magnon splitting measured using BLS. Pseudo-colour two-dimensional plot of the BLS intensity as a function of the excitation and detection frequencies (f and f_{BLS}). The intensity is proportional to the squared amplitude of the FMR mode or to the spin-wave intensity. For each excitation frequency, the applied magnetic field has been adjusted to fulfil the resonance conditions. The solid line indicates the condition of $f_{BLS} = f$, whereas the dashed line corresponds to that of $f_{BLS} = f/2$. Note that spin waves with the half frequency occur only for $f < 3.2$ GHz. The inset is the spin-wave spectrum in YIG with a schematic of the three-magnon splitting. The upper and lower boundaries of the spin-wave manifold correspond to the spin waves propagating perpendicular and parallel to the applied field, as labelled.

Following a simple picture of the three-magnon splitting, where one magnon emits two magnons, one can argue that this process increases the total number of magnons. In a standard quantization scheme, one magnon carries an angular momentum of $\hbar$ (ref. 26) and therefore the three-magnon splitting does not conserve the total angular momentum of the magnetic subsystem. Accordingly, three-magnon splitting is forbidden, if the magnetic system is considered to be isolated, as in the model taking into account only the exchange interaction[26]. This restriction is removed by incorporating the magnetic dipole interaction in the model. In fact, the operator of the angular momentum of the magnetic subsystem alone does not commute with the Hamiltonian describing the magnetic dipole interaction. In contrast, the operator of total angular momentum comprising both the magnetic subsystem and the lattice does commute with this Hamiltonian[27]. As the three-magnon splitting requires the flow of the angular momentum from the lattice, the flow between the lattice and the magnetic subsystem becomes bidirectional, as shown in Fig. 4b. Therefore, in the three-magnon splitting regime, the lattice serves as an additional source of angular momentum flow, which results in the increase of $\Delta M_{\parallel}$ and, consequently, in the enhancement of the spin current across the YIG/Pt interface.

Although the quantum theory of a ferromagnet with both exchange and magnetic dipole interactions has existed for more than 70 years[28,29], a rigorous quantum consideration of the angular momentum exchange between the magnetic subsystem and the lattice due to the dipole interaction is still lacking. Therefore, a quantitative description of the enhancement of spin current due to three-magnon splitting is not possible at the moment. However, even a simple classical consideration of the three-magnon splitting (see Supplementary Information) shows that this process indeed increases $\Delta M_{\parallel}$ and, as a consequence, enhances the spin current across the YIG/Pt interface. The observed enhancement of the spin-current could be also attributed to a higher efficiency in generating spin currents into the normal metal by short-wavelength spin waves than that by the quasi-uniform FMR mode. However, our experiments on excitation of short-wavelength spin waves directly using nonlinear parametric pumping, which are in agreement with results of another group[30], preclude this possibility.

We show that three-magnon splitting in a magnetic insulator, due to angular momentum transfer from the lattice, enhances spin-current emission in the YIG/Pt interface. This enhancement is controlled by changing the frequency and the external magnetic field. These findings shed new light onto the role of nonlinear magnetic dynamics and spin waves in spintronics. In particular, the short-wavelength spin waves, usually considered to be unimportant in conventional microwave electronics, are shown to have potential for spintronic applications. From a fundamental point of view, our findings clearly demonstrate the importance of the magnetic dipole interaction for the exchange of the angular momentum between magnetic and non-magnetic subsystems, and also the importance of the angular momentum conservation law for the analysis of magnetic dynamics.

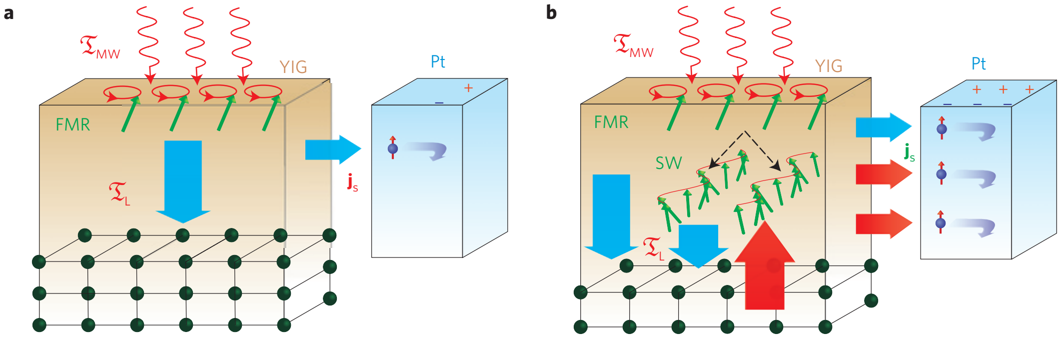

Figure 4 | Schematics of angular momentum flows in the YIG/Pt layered system. a, The case without three-magnon splitting. The external microwave field excites the quasi-uniform FMR mode by transferring the angular momentum into the magnetic subsystem of YIG, $\mathfrak{T}_{MW}$. This flow is directed to the lattice owing to the spin–lattice relaxation in YIG $\mathfrak{T}_L$, and induces a spin current across the YIG/Pt interface $\mathbf{j}_s$. The amplitude of the magnetic precession, which is proportional to $\mathbf{j}_s$, is determined by the equilibrium between the three flows. **b**, The case where three-magnon splitting is allowed. As a result of the three-magnon process the quasi-uniform FMR mode is split into secondary spin waves. To support the splitting, an additional reverse flow of angular momentum from the lattice to the magnetic subsystem is created which enhances the spin current across the YIG/Pt interface (indicated by red arrows). Under these conditions, $\mathbf{j}_s$ is determined by both the amplitude of the quasi-uniform FMR mode and that of secondary spin waves. In both **a** and **b**, FMR denotes the quasi-uniform FMR mode that we excite using microwaves.

Methods

The monocrystalline YIG film, with a thickness of 5.1 μm, was grown on a gallium gadolinium garnet substrate. A 15 nm-thick Pt layer was sputtered on top of the YIG film. The lateral dimensions of the sample were 1.5 × 5 mm. The independently measured Gilbert damping constant of the YIG film was 10^{-4}. As shown in Fig. 1a, the sample was attached to a standard 0.5-mm-wide 50 Ω microstrip transmission line used for broadband excitation of the magnetization dynamics in the YIG film. The excited quasi-uniform FMR mode expands over the entire YIG film owing to the low damping characteristic. The experimental structure was placed in a static magnetic field, $\mathbf{H}_0$, which could be aligned either parallel or perpendicular to the plane of the YIG film. For spin-current detection by the ISHE, two electrodes were attached to the Pt layer, 3.5 mm apart from each other. The electric detection is sensitive to the electric field induced in Pt along the y direction. All the measurements were performed at room temperature.

The magnetization dynamics in the YIG film was studied by two complementary techniques. The quasi-uniform FMR mode was characterized by conventional electronic measurements using the network analyser. Information about the microwave power absorbed in the YIG film was obtained from simultaneous measurements of the power reflected from and transmitted through the microstrip transmission line. In addition, we used BLS spectroscopy in the quasi-backward scattering geometry[19] to access short-wavelength spin waves created in the YIG film as a result of the magnon–magnon relaxation of the directly excited quasi-uniform FMR mode.

Received 15 February 2011; accepted 23 May 2011; published online 3 July 2011

References

1. Maekawa, S. *Concepts in Spin Electronics* (Oxford Univ. Press, 2006).
2. Johnson, M. & Silsbee, R. H. Interfacial charge-spin coupling: Injection and detection of spin magnetization in metals. *Phys. Rev. Lett.* **55,** 1790–1793 (1985).
3. Jedema, F. J., Filip, A. T. & van Wees, B. J. Electrical spin injection and accumulation at room temperature in an all-metal mesoscopic spin valve. *Nature* **410,** 345–348 (2001).
4. Lou, X. *et al.* Electrical detection of spin transport in lateral ferromagnet-semiconductor devices. *Nature Phys.* **3,** 197–202 (2007).
5. Yang, T., Kimura, T. & Otani, Y. Giant spin-accumulation signal and pure spin-current-induced reversible magnetization switching. *Nature Phys.* **4,** 851–854 (2008).
6. Slachter, A., Bakker, F. L., Adam, J-P. & van Wees, B. J. Thermally driven spin injection from a ferromagnet into a non-magnetic metal. *Nature Phys.* **6,** 879–882 (2010).
7. Saitoh, E., Ueda, M., Miyajima, H. & Tatara, G. Conversion of spin current into charge current at room temperature: Inverse spin-Hall effect. *Appl. Phys. Lett.* **88,** 182509 (2006).
8. Kajiwara, Y. *et al.* Transmission of electrical signals by spin-wave interconversion in a magnetic insulator. *Nature* **464,** 262–266 (2010).
9. Kittel, C. *Introduction to Solid State Physics* 7th edn (John Wiley, 1996).
10. Kato, Y. K., Myers, R. C., Gossard, A. C. & Awschalom, D. D. Observation of the spin Hall effect in semiconductors. *Science* **306,** 1910–1913 (2004).
11. Wunderlich, J., Kaestner, B., Sinova, J. & Jungwirth, T. Experimental observation of the spin-Hall effect in a two-dimensional spin–orbit coupled semiconductor system. *Phys. Rev. Lett.* **94,** 047204 (2005).
12. Takahashi, S. & Maekawa, S. Spin current, spin accumulation and spin Hall effect. *Sci Technol. Adv. Mater.* **9,** 014105 (2008).
13. Gurevich, A. G. & Melkov, G. A. *Magnetization Oscillations and Waves* (CRC, 1994).
14. Sandweg, C. W., Kajiwara, Y., Ando, K., Saitoh, E. & Hillebrands, B. Enhancement of the spin pumping efficiency by spin wave mode selection. *Appl. Phys. Lett.* **97,** 252504 (2010).
15. Kittel, C. On the theory of ferromangetic resonance absorption. *Phys. Rev.* **73,** 155–161 (1948).
16. Tserkovnyak, Y. & Brataas, A. Enhanced Gilbert damping in thin ferromagnetic films. *Phys. Rev. Lett.* **88,** 117601 (2002).
17. Tserkovnyak, Y., Brataas, A. & Bauer, G. E. Dynamic stiffness of spin valves. *Phys. Rev. B* **67,** 140404 (2003).
18. Ando, K. & Saitoh, E. Inverse spin-Hall effect in palladium at room temperature. *J. Appl. Phys.* **108,** 113925 (2010).
19. Demokritov, S. O., Hillebrands, B. & Slavin, A. N. Brillouin light scattering studies of confined spin waves: Linear and nonlinear confinement. *Phys. Rep.* **348,** 441–489 (2001).
20. Ordóñez-Romero, C. L. *et al.* Three-magnon splitting and confluence processes for spin-wave excitations in yttrium iron garnet films: Wave vector selective Brillouin light scattering measurements and analysis. *Phys. Rev. B* **79,** 144428 (2009).
21. Schultheiss, H. *et al.* Direct current control of three magnon scattering processes in spin-valve nanocontacts. *Phys. Rev. Lett.* **103,** 157202 (2009).
22. Kalinikos, B. A. & Slavin, A. N. Theory of dipole-exchange spin wave spectrum for ferromagnetic films with mixed exchange boundary conditions. *Physica C* **19,** 7013–7033 (1986).
23. Wigen, P. E. *Nonlinear Phenomena and Chaos in Magnetic Materials* (World Scientific, 1994).
24. Khitun, A., Bao, M. & Wang, K. L. Spin wave magnetic nanofabric: A new approach to spin-based logic circuitry. *IEEE Trans. Mag.* **44,** 2141–2151 (2008).
25. Einstein, A. & de Haas, W. J. Experimenteller Nachweis der Ampereschen Molekularstörme, Verhandlungen. *Dtsch. Phys. Gesellschaft.* **17,** 152–170 (1915).
26. Bloch, F. Zur Theorie des Ferromagnetismus. *Z. Phys.* **61,** 206–219 (1930).
27. Bloembergen, N. S., Shapiro, P. S., Pershan, O. & Artman, Cross-relaxation in spin systems. *Phys. Rev.* **114,** 445–459 (1959).
28. Holstein, T. & Primakoff, H. Field dependence of the intrinsic domain magnetization of a ferromagnet. *Phys. Rev.* **58,** 1098–1113 (1940).
29. Majlis, N. *The Quantum Theory of Magnetism* 2nd edn (World Scientific Publishing, 2007).
30. Sandweg, C. W. *et al.* Spin pumping by parametrically excited exchange magnons. *Phys. Rev. Lett.* **106,** 216601 (2011).

Acknowledgements

The authors thank A. Slavin, E. Saitoh, K. Ando, K. Harii and Y. Tserkovnyak for their valuable discussions. H.K. is grateful to the Royal Society for their financial support via TG102227. S.O.D. acknowledges helpful discussions with B. Koopmans on the conservation of angular momentum in ferromagnets. Work in Münster has been supported by the Deutsche Forschungsgemeinschaft and by the European Union through the STREP Project Master NMP3-SL-2008-212257.

Author contributions

Sample preparation: H.K., O.D. and D.F.; measurement and data analysis: O.D., H.K. and V.E.D.; interpretation and theoretical calculation: S.O.D. and H.K.; manuscript writing: S.O.D., H.K., V.E.D. and A.J.F. This project was initiated and managed by H.K. and S.O.D.

Additional information

The authors declare no competing financial interests. Supplementary information accompanies this paper on www.nature.com/naturematerials. Reprints and permissions information is available online at http://www.nature.com/reprints. Correspondence and requests for materials should be addressed to H.K.